Dionys Van Gemert*, Eleni-Eva Toumbakari, Sven Ignoul and Kris Brosens

Consolidation and Strengthening of Historical Masonry by Means of Mineral Grouts: Modeling Structural Behavior of Grouted Three-Leaf Masonry

Abstract: Development of mineral grouts for consolidation and strengthening of historical masonry was discussed in Ref. [1]. The properties of the injection grout must counteract the elements that initiate the failure mechanism of multiple leaf historical masonry and lead to its collapse. This paper presents a macro-approach to model the structural behavior of three-leaf masonry. A global approach is used, based on the properties and the behavior of the external leafs, in combination with the properties and behavior of the central core of the three-leaf wall. Evaluation of the models is made by comparison with experimental data.

Keywords: three-leaf masonry, collapse mechanism, consolidation, injection grouts, modeling, global approach

DOI 10.1515/rbm-2015-0005

1 Introduction

Special injection grouts and injection technologies have been developed since the 1990s to enable an appropriate consolidation of degraded historical masonry [1]. Degradation phenomena appear in the mortar as well as in the stones. As a result, the quality of both, and the quality of the bond between stone and mortar diminish. The mechanical action on the masonry walls normally causes distributed vertical compressive stresses in the masonry, but at every discontinuity such as cracks, holes and pores, interfaces between stones and mortar, also tensile stresses will appear. The tensile stresses can cause cracking or micro-cracking in the stones, the mortar or in the bond between them. Keeping in mind that tensile stresses are causing masonry failure, it is evident that every strengthening method must introduce elements or systems, capable of withstanding these tensile stresses. Grouted anchors and injected grouts are potential methods, but each of them has its specific application fields, and design will always be problem oriented.

As shown in Ref. [1] discontinuities and holes initiate crack formation in the masonry. Therefore, strengthening or consolidation must remove such discontinuities. In multiple leaf masonry, the internal core masonry has a lower stiffness than the external paraments, causing overloading of the paraments: consolidation must enhance stiffness of the core. Final collapse in multiple leaf masonry is linked to buckling of the paraments: strengthening and consolidation must provide a better adhesion between parament and core or must provide mechanical anchoring of paraments to core. The failure plane is diagonally through the masonry: the consolidation must provide improved strength (cohesion) of the mortar, by which the core masonry gets enhanced shear strength.

The different strengthening and consolidation principles are as follows:

- filling of holes and cracks
- enhancement of stiffness of core masonry
- preventing buckling of paraments
- enhancement of cohesion and strength of core masonry
- improving homogeneity of the masonry as a whole.

Grouting intends to enhance the structural behavior of the masonry, considered as a composite material of high complexity. To model the structural behavior of grouted masonry based on a micro-approach, a great number of parameters describing the interactions between all the components remains unknown. Therefore, this paper uses a global approach based on parameters that relate to the whole masonry, to the injection grout, as well as to

***Corresponding author: Dionys Van Gemert,** Triconsult nv, Lindekensveld 5 bus 3.2, B-3560 Lummen, E-mail: dionys.vangemert@bwk.kuleuven.be
Eleni-Eva Toumbakari, Ministry of Culture, Vas. Konstantinou 2 – Maroussi, 151 22 Athens
Sven Ignoul, Kris Brosens, Triconsult nv, Lindekensveld 5 bus 3.2, B-3560 Lummen

parameters that relate to the core and the paraments as components of the masonry.

2 Global approach of mechanical strength after consolidation [2]

The strengthening effect of masonry in real projects is only poorly documented in literature [3, p. 229], and results show a wide spread. This may not be a surprise, because each monumental masonry has its unique and specific properties and composition. Therefore, experimental results have only guiding importance, in indicating which elements are important in design of masonry consolidation. For injection grouts these are: fluidity, stability, bending strength as measure for bond.

Some researchers proposed theoretical models to estimate strength after consolidation. All such models need a number of data on the existing masonry as a basis for the prediction model. However, it will mostly be impossible to collect reliable and representative data on the site. A simple, but interesting model for the strength of three-leaf masonry has been proposed by E. Vintzileou and T.P. Tassios [2]:

$$f_{wc,s} = \left(\frac{V_{\text{ext}}}{V}\right).f_{\text{ext}} + \left(\frac{V_{\text{inf}}}{V}\right).f_{\text{inf},s} \tag{1}$$

The following notations are used in eq. (1):
- $f_{wc,s}$: compressive strength of injected three-leaf masonry
- f_{ext}: compressive strength of parament
- $f_{\text{inf},s}$: compressive strength of injected core masonry (infill)
- V: total volume of masonry
- V_{ext}: volume of paraments
- V_{inf}: volume of infill core masonry

It concerns a simple rule of volumes, assuming that the global strength is the sum of relative strengths of paraments and core. Because the strength of core masonry before injection is always quite low, Vintzileou and Tassios proposed to neglect the original strength of the infill and to use the following expression to calculate this strength only on the basis of grout strength f_{cg}:

$$f_{\text{inf},s} = 1.25 f_{cg}^{0.5} \tag{2}$$

The results of the test wallets were used to evaluate the above formulas (Table 1). The strongest grout should have the most marked strengthening effect. The volume fractions in the test wallets are about 45% parament and 55% core masonry. Assuming that the core strength is about zero before injection, and assuming that the parament is not affected by the injection, the strength increases after injection can be calculated with the second part of formula (1) only:

$$\Delta f_{wc,s} = \left(\frac{V_{\text{inf}}}{V}\right).f_{\text{inf},s} \tag{3}$$

The comparison indicates that the proposed formulas are not reliable, and that the compressive strength of the grout is not the determining factor for the consolidation effect. For the brick wallets BC, the greatest strength increase is found for BC4 and BC5, injected with the weakest grout.

For the limestone wallets, the stronger grout in SC2 does not bring a significantly higher strength increase compared to the weaker grout in SC1.

A better correspondence is to be expected between the strength increase of the injected three-leaf masonry and the flexural strength of the injection grout. Table 2 collects some available data.

The grout in brick wallet BC3 and in stone wallet SC3 was a pure cement-based grout [4]. The other grouts contained 30 wt.% of cement, and a lime:pozzolan ratio of 1:3. The grout for brick wallet BC2 contained 10 wt.% of silica fume. Contrary to what could be expected, the relation between the flexural strength of the injection grout and the strength increase of grouted masonry wallets is not clear.

Table 1 Comparison between model and experiment. Strength values at 60 d on samples taken during grouting

Wallet	Compressive strength of grout [3] MPa	$\Delta f_{wc,s}$ experimental [1, Table 3] MPa	$\Delta f_{wc,s}$ model, formula (3) MPa
BC2	11.9	0.74	2.37
BC3	18.0	0.82	2.92
BC4	6.6	0.82	1.77
BC5 (t.l.)	6.6	1.58	1.77
SC1	6.6	1.23	1.77
SC2	18.0	1.29	2.33
SC3 (t.l.)	6.6	0.86	1.77
SC4	6.6	0.58	1.77

Table 2 Strength values of grouts versus strength increase of grouted masonry. Grout strengths from Ref. [3]

Wallet	Compressive strength of grout MPa	Flexural strength of grout MPa	Shear bond strength τ_u MPa	$\Delta f_{wc,s}$ experimental [1] Table 3 MPa
BC2	11.9	2.0	1.12	0.74
BC3	18.0	4.8	1.19	0.82
BC4	6.6	1.9	0.83	0.82
BC5 (t.l.)	6.6	1.9	0.83	1.58
SC1	6.6	1.9	0.83	1.23
SC2	18.0	4.8	1.19	1.29
SC3 (t.l.)	6.6	1.9	0.83	0.86
SC4	6.6	1.9	0.83	0.58

Therefore, a model was developed which takes into account the shear bond strength τ_u of the grout to a brick or to a stone substrate.

3 Modeling the mechanical behavior of three-leaf wall [3, 5]

A suitable model must at least be able to "predict" the experimentally observed and measured stress–strain evolution of the grouted three-leaf wallets. The vertical behavior of a three-leaf masonry wall is schematically shown in Figure 1.

Figure 2 shows a simplified model, in which the shear stress distribution is assumed to be linear.

It is assumed that in the starting situation, the axial load N on the wallet is carried by the two external leaves only. Their summed cross section is $2A_e$ with width b. This assumption is based on: the different deformability of the external and the internal leaves; different shrinkage behavior of the internal leaf, with higher mortar content; horizontal micro-cracks in the core at the interface between external and internal leaves.

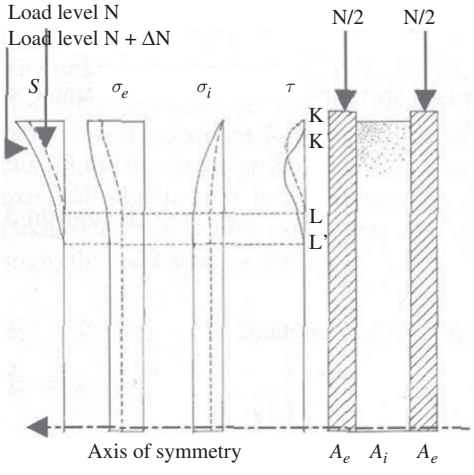

Figure 1 Vertical and shear stresses between parament and core, before and after reaching τ_u [3]

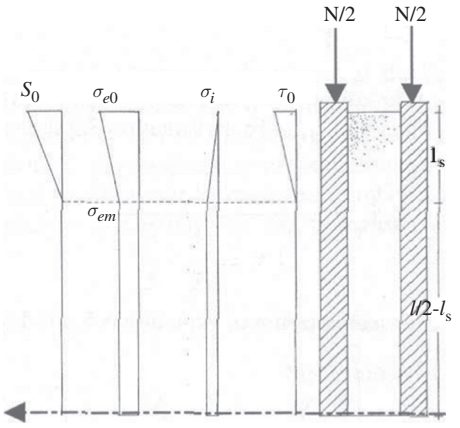

Figure 2 Simplified model, with linear stress distributions [3]

Collaboration of internal and external leaves is therefrom only possible if shear stresses are mobilized between the stiffer external leafs and the more deformable core, as shown in Figure 1, and schematized in Figure 2.

Shear stresses are only acting in a reduced area of length l_s (Figure 2), as it is well known from shear stress distributions in lap-joints [6]. Once the bond stress developing at the edge exceeds the bond strength τ_u of the system, the bond breaks locally. This failure imposes a displacement of the active area KL in Figure 1 to K'L'. New shear stresses are then mobilized but the active shear region keeps the same length l_s. Local bond failure and the consequent shift of the active shear length l_s occur when the slip s_0 between the external leaf and the internal core exceeds a certain limit value s_u (Figure 3).

The values (s_u, τ_u) for the brick-grout and the limestone-grout systems have been experimentally determined [3]. Relevant data are given in Ref. [1] (Tables 1 and 2). For other stones and grout systems, such data can also easily been determined in a shear box (Figure 4).

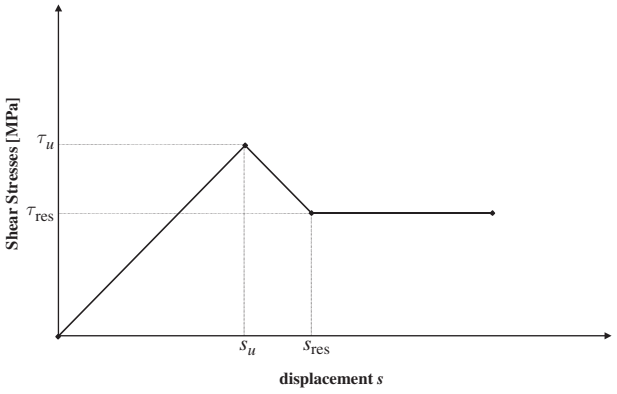

Figure 3 Shear stress–slip relation for grout–substratum interface

Condition for zero slip at point L (Figure 2):

The axial displacements of external leaves (left part in expression (4)) and internal leaf (right part) are equal below point L: the slip s_L at point L is zero.

$$s_L = 0 : \frac{N - \tau_0 l_s b}{2A_e E_e}\left(\frac{l}{2} - l_s\right) = \frac{\tau_0 l_s b}{A_i E_i}\left(\frac{l}{2} - l_s\right) \tag{4}$$

ensuing that

$$\frac{N}{A_e E_e} = \tau_0 l_s b\left(\frac{1}{A_e E_e} + \frac{2}{A_i E_i}\right) \tag{5}$$

- A_e is cross section area of external leaf;
- A_i is cross section area of internal core;
- E_e is modulus of elasticity of external leaf;
- E_i is modulus of elasticity of core;
- l is length (height) of wall(et).

Slip at beginning K of load transfer length l_s

$$s_0 = \frac{l_s}{E_e}\frac{1}{2}\left(\frac{N}{2A_e} + \frac{N - \tau_0 l_s b}{2A_e}\right) - \frac{l_s}{2E_i} \cdot \frac{\tau_0 l_s b}{A_i} \tag{6}$$

Shear stress–slip behavior (Figure 3)

$$\tau_0 = \frac{\tau_u}{s_u} \cdot s_0 \tag{7}$$

The above equations contain the known parameters N, B, A_e, A_i, E_e and E_i. The deformation moduli E_e and E_i have to be determined experimentally or taken from literature. If no experimental data are available, some correlating expressions can be used, by which the moduli are approximately calculated from the strengths of external leaves and internal core. However, if strengths are determined experimentally, measuring the corresponding elongations also provides the moduli.

$$\begin{aligned} E_e &= k_e \cdot f_{c,e} \\ E_i &= k_i \cdot f_{c,i} \end{aligned} \tag{8}$$

in which

- $f_{c,e}$ is compressive strength of external leaf
- $f_{c,i}$ is compressive strength of core masonry.

Equation (5) gives $\tau_0 l_s b$

$$\tau_0 l_s b = \frac{N}{1 + 2\frac{A_e}{A_i} \cdot \frac{E_e}{E_i}} \tag{9}$$

Combining expressions (6) and (9) gives an expression for s_0

$$s_0 = \left(\frac{N}{A_e E_e} - \frac{N}{1 + 2\frac{A_e}{A_i} \cdot \frac{E_e}{E_i}} \cdot \left(\frac{1}{2A_e E_e} + \frac{1}{A_i E_i}\right)\right) \cdot \frac{l_s}{2} \tag{10}$$

Putting s_0 from expression (7) and l_s from eq. (5) into eq. (10) yields an expression for the value of the developing shear stress τ_0:

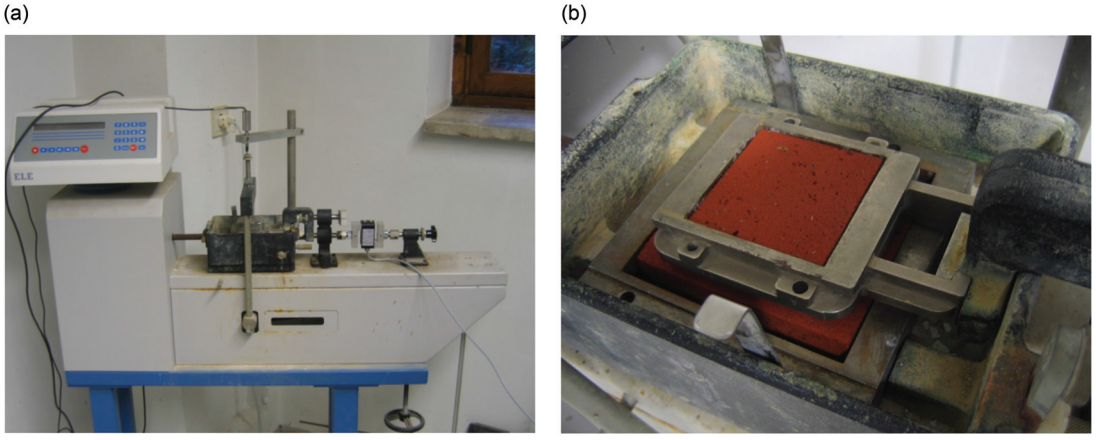

Figure 4 (a) Shear box. (b) Specimen for brick-grout shear bond testing

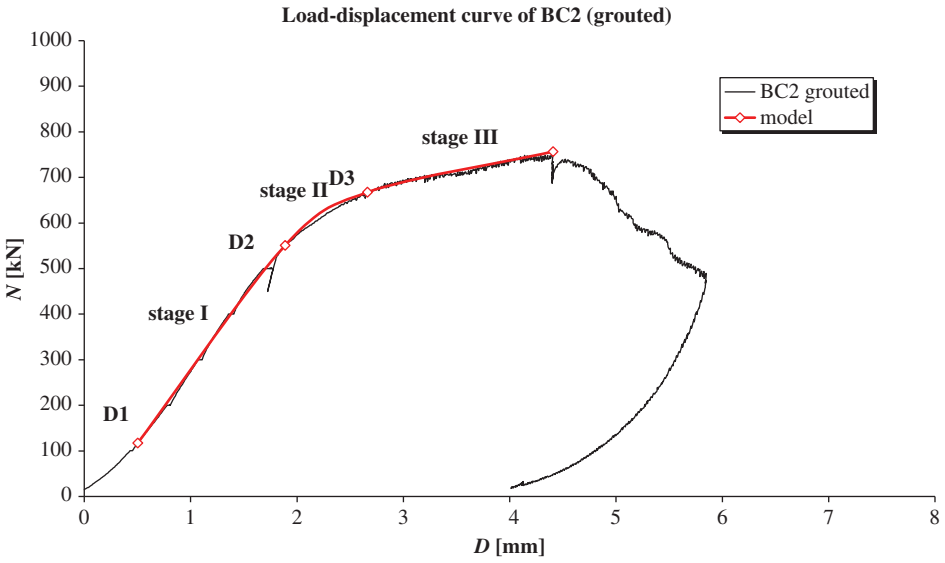

Figure 5 Load–displacement curve of wall BC2 (grouted), with the division points *D*1, *D*2 and *D*3 used in the model

$$\tau_0^2 = N \cdot \frac{\tau_u}{2b \cdot s_u} \cdot \frac{1}{\left(1 + 2 \cdot \frac{A_e}{A_i} \cdot \frac{E_e}{E_i}\right)} \cdot \left(\frac{N}{A_e E_e} - \frac{N}{1 + 2\frac{A_e}{A_i} \cdot \frac{E_e}{E_i}} \cdot \left(\frac{1}{2A_e E_e} + \frac{1}{A_i E_i}\right)\right) \tag{11}$$

If all the geometrical and material data are known, eq. (11) gives the normal force N at which τ_0 reaches its limit value τ_u, and thus the value at which debonding starts.

If no data on strength of leaves and global wall are available, the following conditions can be applied to make appropriate estimations:

Condition 1: equivalence of forces at limit state

$$2A_e \cdot f_{c,e} + A_i \cdot f_{c,i} = (2A_e + A_i) \cdot f_{wc} \tag{12}$$

Condition 2: The vertical deformation ε_z is the same for all three leaves, at each loading stage:

$$\begin{aligned} &2A_e \cdot \sigma_{c,e} + A_i \cdot \sigma_{c,i} = (2A_e + A_i) \cdot \sigma_{wc} \Rightarrow \\ &2A_e \cdot \varepsilon_z \cdot E_{c,e} + A_i \cdot \varepsilon_z \cdot E_{c,i} = (2A_e + A_i) \cdot \varepsilon_z \cdot E_{wc} \Rightarrow \\ &2A_e \cdot E_{c,e} + A_i \cdot E_{c,i} = (2A_e + A_i) \cdot E_{wc} \end{aligned} \tag{13}$$

Expressions (12) and (13) are helpful in estimating the missing mechanical properties of the separate leaves.

It must be recognized that the choice of the value for some parameters may be difficult: the k-factors in expressions (8) are material and load dependent and can also be influenced by the geometrical length/width/depth ratios. Besides, strength and deformation parameters depend on damage accumulated in the materials. Reasonable estimations can be made on the basis of available literature data. However, good engineering judgment will always be needed.

The simple model above was used to simulate the behavior of the wallets under increasing vertical load. As an example, the results for wallet BC2 are shown hereafter (Figure 5).

In this case, and with the experimental curve available, it was easy to choose the division points D at locations with clear change of curvature.

The geometrical data and shear properties of the system are given in Table 3.

Table 3 System properties for wallet BC2

Property	Value
A_{tot} (mm²)	240,000
A_e (mm²)	54,000
A_i (mm²)	132,000
t_e (mm)	90
t_i (mm)	220
b (mm)	600
τ_u (MPa)	0.67
s_u (mm)	0.38
f_{wo} (MPa) (not grouted)	2.41 [1, Table 3]
f_{wc} (MPa) (grouted)	3.15 [1, Table 3]

The experimental data, corresponding to the three division points, are given in Table 4.

For the calculations of the moduli and strengths of the individual leaves, it was assumed that inside the three stages of loading considered, the moduli of elasticity and the compressive strengths remained constant. A satisfactory fit was found for the values listed in Table 5.

Table 4 Experimental data, corresponding to the division points

		D1	*D2*	*D3*
D_1	mm	0.5026	1.8884	2.6616
$\varepsilon_{v,1}$	‰	0.42	1.57	2.22
N_1	kN	117.2	551.0	667.8
σ_1	MPa	0.49	2.30	2.78
D_2	mm	1.8884	2.6616	4.4097
$\varepsilon_{v,2}$	‰	1.57	2.22	3.67
N_2	kN	551.0	667.8	756.7
σ_2	MPa	2.30	2.78	3.15
E_{wall} (tangent)	MPa	1,565.0	755.7	254.2

The strength $f_{c,e}$ of the external leaf was found from the compressive test on the non-grouted wallet BC2, assuming that the core had no strength at all. Grouting will nearly not affect the strength of the external leaf, ensuing that $f_{c,i}$ can be derived from eq. (12). With the values of Table 5, the shear force transfer length in phase I can be calculated with expression (9):

$$l_s = 385\,\text{mm}.$$

With the values, listed in Table 5, the load–deformation curve of BC2 can be reconstructed. Moreover, these values can also be used for walls with similar material compositions, but different geometry.

The above calculations are easy, because enough experimental data are available. If that is not the case, a test injection will provide the necessary technological and mechanical information.

4 Test injection

In most projects, it will be advisable or even necessary to execute a test injection to determine the best grout composition and to estimate the attainable consolidation effect in the specific masonry.

A number of small test zones of the masonry can be marked out on before by means of an injection with expansive polyurethane resin. As an example, the injection test made within the restoration project of the monumental "Oud Gemeentehuis" (Old Community Hall) at Opglabbeek (B) is shown in Figures 6–9. The original brick masonry was very weak, because of using very weak original brick material, as well as by environmental degradation, hidden by an external, cement-based rendering. This cement-based rendering even aggravated the deterioration and pulverization of the masonry, by hindering drying of the masonry and accelerating freezing of the entrapped water.

Figure 6 Monument "Oud Gemeentehuis" at Opglabbeek (B)

In this case, three injection zones were isolated, in which three types of grouts were injected: a binary lime–cement grout; an epoxy resin; a micro-cement. Simple volume measurements allow to determine the grout consumption that can be expected in the specific masonry.

After injection, Figure 9, test samples can be cored out from the injected zones and the desired samples can be prepared to check the consolidation result (Figures 10 and 11).

In this case the consolidation by epoxy resin proved to be very efficient and homogeneous and was chosen for consolidation of column-like masonry zones in the most

Table 5 Mechanical properties of external and internal leaves of BC2, derived from model

External leaf					Internal leaf
$f_{c,e}$ Mpa	k_e	E_e MPa	$f_{c,i}$	k_i	E_i
		Level I			Level I
5.36	466	2,500	1.35	592	800
		Level II			Level II
5.36	280	1,500	1.35	109	147

Figure 7 Application of a temporary protective coating at the outside of the test zone in the wall (Project Community Hall Opglabbeek, 2008)

Figure 10 Cored test samples

Figure 8 Marking out of an injection zone with expansive PU resin

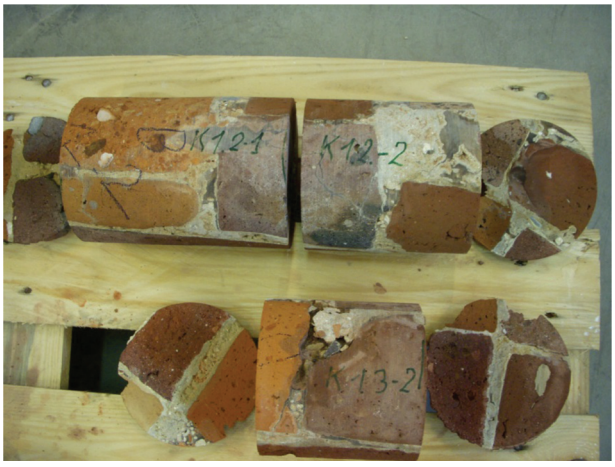

Figure 11 Preparation of test samples from cores, for visual and mechanical investigation

Figure 9 Injection of a test zone

loaded areas. Results of compressive strength of injected masonry are presented in Table 6. In this case, the mechanical performance of the resin injected masonry is about double the one of the masonry, injected with mineral grout.

Although the consolidation results of lime–cement grout and micro-cement grout were similar, the masonry in between the consolidated column zones was consolidated by means of a micro-cement grout because of the easier mixing procedure.

5 Conclusions

Modeling the strengthening effect of a consolidation grouting is a complex task. Many factors influence the strengthening result. Not only the type and quality of the original masonry

Table 6 Results of three types of grouting in massive brick masonry

Specimen	Height of specimen (mm)	Density (kg/m³)	Compress.Strength (N/mm²)	Remarks
Grouted with epoxy resin (±100 l/m³)				
K1.1	237.3	1,753	6.4	
K1.2-1	162.8	1,813	9.1	
K1.2-2	121.6	1,798	22.6	Perfect filling of voids
K1.3-1	185.8	1,783	8.1	
K1.3-2	112.1	1,779	11.4	
Grouted with lime-cement grout (±40 l/m³)				
K2.1	199.1	1,787	3.6	
K2.4	150.6	1,840	4.0	
Grouted with micro-cement grout (±70 l/m³)				
K3.1-1	168.0	1,836	7.1	Brick part over full height
K3.2	210.4	1,841	4.4	
K3.3-1	181.6	1,840	3.2	
K3.3-2	134.7	1,824	4.4	

are important but also the grout properties, the interaction between grout and brick or stone, its interaction with the original mortar, the void ratio of the original masonry, the filling ratio of the grout in the voids. This paper describes some models, proposed on the basis of logical engineering considerations. But comparison with experimental data shows that most models are not reliable. Up to now, models can only be used as indicators of structural improvement. If more detailed information is needed because of the precarious safety situation of the historical masonry or the historical building, test injections should be executed to determine the best grout composition and to estimate the consolidation effect.

References

1. Van Gemert D, Ignoul S, Brosens K, Toumbakari E-E. Consolidation and strengthening of historical masonry by means of mineral grouts: grout development. Restor Build Monuments 2015;21:29–46.
2. Vintzileou E, Tassios TP. Three-leaf stone masonry strengthening by injecting cement-grouts. J Struct Eng 1995;121:848–56.
3. Toumbakari E. Lime-pozzolan-cement grouts and their structural effects on composite masonry walls. PhD thesis K.U. Leuven 2002, 310 pp.
4. Van Gemert D, Toumbakari E-E, Schueremans L. Konstruktive injektion von historischem mauerwerk mit mineralisch- oder polymergebundenen mörteln. Int J Restor Build Monuments 1999;5:73–98.
5. Toumbakari E, Van Gemert D, Tassios TP, Vintzileou E. Experimental investigation and analytical modeling of the effect of injection grouts on the structural behaviour of three-leaf masonry walls In: Modena C, Lourenco PB, Roca P, editors. Structural analysis of historical constructions. Rotterdam: Balkema Publisher, 2005. ISBN 04 1536 379 9, 707–717
6. Van Gemert D. Force transfer in epoxy bonded steel-concrete joints. Int J Adhes Adhes 1980;2:67–72.